Hindawi Publishing Corporation
Journal of Nanomaterials
Volume 2015, Article ID 481087, 9 pages
http://dx.doi.org/10.1155/2015/481087

Research Article

Electronic and Optical Properties of Small Hydrogenated Silicon Quantum Dots Using Time-Dependent Density Functional Theory

Muhammad Mus-'ab Anas and Geri Gopir

School of Applied Physics, Faculty of Science and Technology, Universiti Kebangsaan Malaysia, 43600 Bangi, Selangor, Malaysia

Correspondence should be addressed to Muhammad Mus-'ab Anas; mus_physics@yahoo.com

Received 29 April 2015; Revised 31 August 2015; Accepted 31 August 2015

Academic Editor: Bin Dong

This paper presents a systematic study of the absorption spectrum of various sizes of small hydrogenated silicon quantum dots of quasi-spherical symmetry using the time-dependent density functional theory (TDDFT). In this study, real-time and real-space implementation of TDDFT involving full propagation of the time-dependent Kohn-Sham equations were used. The experimental results for SiH_4 and Si_5H_{12} showed good agreement with other earlier calculations and experimental data. Then these calculations were extended to study larger hydrogenated silicon quantum dots with diameter up to 1.6 nm. It was found that, for small quantum dots, the absorption spectrum is atomic-like while, for relatively larger (1.6 nm) structure, it shows bulk-like behavior with continuous plateau with noticeable peak. This paper also studied the absorption coefficient of silicon quantum dots as a function of their size. Precisely, the dependence of dot size on the absorption threshold is elucidated. It was found that the silicon quantum dots exhibit direct transition of electron from HOMO to LUMO states; hence this theoretical contribution can be very valuable in discerning the microscopic processes for the future realization of optoelectronic devices.

1. Introduction

Current nanostructures, including clusters, biomolecules, and molecular nanodevices, have become the core of many fundamental and technological research projects. The study of static and dynamic electron-electron correlation makes it possible to characterize the electronic, structural, and bonding properties in nanostructure regime. Additional to that, its necessity is also related to the optical, electronic, and time-resolved spectroscopies. Since the structural and electronic properties of nanoparticle, in particular silicon quantum dots, are absolutely sensitive to the changes of atomic configuration, impurities, and doping effect [1], these challenges urged researchers to understand the phenomena involved specifically from quantum mechanics perspective. One can obtain the electronic structure information from the optical analysis; in particular, the optical response of the quantum dots will provide informative view of its dependency on their size and geometrical structure. This is an important feature, since the determination of the structure is, in general, a very sensitive task, either for prototype construction or for sophisticated relaxation of total energy minimization. Furthermore, the knowledge of the geometrical structure for modeling is highly required from solid state physics as a basis for understanding many of the properties of the nanostructure material.

Relatively large quantum dots consisting of thousands of atoms need very high computational cost in order to solve their many-body problem wave functions. Here, the importance of parallel processing combined with perfect computational strategy urged researchers to seek more efficient alternatives to overcome these challenges. Real-space grids are a powerful alternative tool for the simulation of electronic systems. One of the main advantages of this approach is the flexibility and simplicity of working directly in real space where the different fields are discretized on a grid, combined

with competitive numerical performance and great potential for parallelization. In this study, this paper is divided into two main parts. In the first section, the electronic properties of ground state hydrogenated silicon quantum dots using density functional theory by three different methods will be briefly reviewed. This comparison step is taken to act as a benchmark for further study of the optical spectra using the time-dependent density functional theory (TDDFT) [2, 3]. Secondly, the basic framework of TDDFT is used for the calculation of the quantum dot optical spectra. This framework is applied in real space by the first principles code of OCTOPUS [4] that allows the study of electron-ion dynamics of many-electron systems under the presence of arbitrary external perturbation.

In particular, this paper will investigate the effect of quantum confinement on the energy gap of hydrogen passivated silicon quantum dots with various sizes. In this aspect, this study is focused to compute the energy gap and optical absorption spectra as a function of dot size, in order to examine the behavior of optical gap under quantum confinement effect. This study is also focused to get brief insight at the microscopic level of the electron transition and bonding characteristic of the dots, identified from the distribution of the highest occupied molecular orbitals (HOMO) and the lowest unoccupied molecular orbitals (LUMO) isosurface.

Since quite a number of computational studies on silicon quantum dots were reported earlier, calculation results were compared with previous studies as a benchmark of this extended study conducted. Serious selection of computational method and parameters is very important in order to achieve ideal counter and balance between efficiency and computational cost. Before the calculation starts, important related background study for comparison purpose was conducted. These results were compared with Zdetsis et al. [8], where the same orbital basis-set representation was used, but it was different in parameters. Models for various prototype structures were done, especially for the structure below 1.8 nm. Those models also covered the missing structure reported from Hirao and Uda [6] DFT calculation with the same exchange-correlation functional. Those possible prototypes were discovered during structural construction while preserving quasi-spherically structured quantum dots.

Computational works done by Onida and Andreoni [12], Xue Jiang et al. [13], and Vasiliev [14] were reported by many; these reports covered small quantum dots (below 0.8 nm) which also considered as small clusters were used as early benchmark for the calculation conducted in this study. Since larger quantum dots (~1.6 nm) fell into quantum confinement regime of electron movement, it was decided to extend this study and analyze computationally atomistic *ab initio* method to understand quantum behavior of electron under confinement region, where all electron and orbital were taken into account. Using the computational facilities available, combined with good calculation approach, this study is capable of analyzing time-dependent optical properties of silicon quantum dots under 1.6 nm in diameter corresponding to 160 atoms ($Si_{87}H_{76}$).

2. Theoretical Background

Time-dependent density functional theory (TDDFT) [2, 3] can be used to obtain the optical spectra from relaxed geometries. TDDFT is an exact reformulation of time-dependent quantum mechanics, in which the fundamental variable is no longer the many-body wave function but the time-dependent density. TDDFT is an extension of DFT with the time-dependent domain to describe what happens when a time-dependent perturbation is applied. For the sake of completeness, the essentials of this method can be summarized explicitly. In TDDFT, the basic variable is the one electron density $n(r,t) = \sum_{i=1}^{N} |\varphi_i(\mathbf{r},t)|^2$, which is obtained with the help of a fictitious system of noninteracting electrons, the Kohn-Sham system. The interacting system can be represented with the time-dependent Kohn-Sham orbitals $\varphi_i(\mathbf{r},t)$, using the time-dependent Kohn-Sham equation,

$$i\frac{\delta}{\delta t}\varphi_i(\mathbf{r},t) = \left[-\frac{\nabla^2}{2} + V_{\mathrm{KS}}(\mathbf{r},t)\right]\varphi_i(\mathbf{r},t). \quad (1)$$

The Kohn-Sham potential $V_{\mathrm{KS}}(\mathbf{r},t)$ is defined as

$$V_{\mathrm{KS}}(\mathbf{r},t) = V_{\mathrm{ext}}(\mathbf{r},t) + V_H(\mathbf{r},t) + V_{\mathrm{xc}}(\mathbf{r},t), \quad (2)$$

where $V_{\mathrm{ext}}(\mathbf{r},t)$ is the external potential, $V_H(\mathbf{r},t)$ is Hartree potential, and $V_{\mathrm{xc}}(\mathbf{r},t)$ is the exchange and correlation potential. In this study, the adiabatic local density approximation (ALDA) for the whole simulation was used, where it is mapped from homogenous electron gas (HEG),

$$V_{\mathrm{xc}}^{\mathrm{ALDA}}(\mathbf{r},t) = V_{\mathrm{xc}}^{\mathrm{HEG}}(n)\Big|_{n=n(\mathbf{r},t)}. \quad (3)$$

Since the exchange and correlation functional is the heart of density functional theory calculation, it is very important that this crucial part be reviewed before proceeding into the further calculation. There are numbers of publications that explore the reliability of various exchange-correlation functionals used to study electronic properties of silicon quantum dots. As reported by Zdetsis et al. [8], result of calculated energy gap using semiempirical hybrid exchange-correlation functional (B3LYP) overestimated the experimental value especially for the dots with diameter below 1.8 nm, while it is accurate for larger structure around 1.8–2.0 nm. Even though this hybrid functional was optimized by chemist to overcome the weaknesses of coulomb potential in local density approximation (LDA) for molecular structure study, here the reliability of LDA functional was demonstrated to explore the electronic and optical properties of small sized silicon quantum dots as presented in this paper. This is also confirmed by earlier computational research reported by Hirao and Uda [6], where the LDA functional is also used to study hydrogenated silicon quantum dots. For the sake of reducing computational cost while maintaining its accuracy, it was found that LDA results were acceptable to study quantum dot sizes silicon semiconductor as benchmarked with reported experimental results.

Next, the absorption spectrum was calculated using the explicit propagation of the time-dependent Kohn-Sham

equations. Throughout this approach, the system was first excited from its ground state by applying a delta electric field, $E_0\delta(t)\mathbf{e}_m$. The unit vector $\mathbf{e}_m$ determines the polarization direction of the electric field and E_0 is its magnitude, which must be small enough if one is interested in linear response. The reaction of the noninteracting Kohn-Sham system caused by the perturbation can be readily computed. The mechanism described that each ground state Kohn-Sham orbital $\varphi_i^{\mathrm{GS}}(\mathbf{r})$ instantaneously phase-shifted, where $\varphi_i(\mathbf{r}, t = 0^+) = e^{iE_0\mathbf{e}_m\cdot\mathbf{r}}\varphi_i^{\mathrm{GS}}(\mathbf{r})$. The Kohn-Sham equations are then propagated forward in real time, and by then the time-dependent density $n(\mathbf{r}, t)$ can be computed. The induced dipole moment variation is an explicit functional of the density:

$$\delta\mathbf{D}^m(t) = \delta\left\langle\widehat{\mathbf{R}}\right\rangle(t) = \int d^3r\,[n(\mathbf{r},t) - n(\mathbf{r},t=0)]\,\mathbf{r}. \quad (4)$$

The super index m indicates that the perturbation has been applied along the mth Cartesian direction. Then, the component of the dynamical dipole polarizability tensor $\alpha(\omega)$ is directly related to the Fourier transform of the induced dipole moment function:

$$\alpha_{mn} = \frac{\delta D_n^m(\omega)}{E_0}. \quad (5)$$

The spatially averaged absorption cross section is trivially obtained from the imaginary part of the dynamical polarizability:

$$\sigma(\omega) = \frac{4\pi\omega}{c}\,\mathrm{Im}\left[\alpha(\omega)\right], \quad (6)$$

where α as the function of ω is the spatial average, or trace, of the α_{mn} tensor

$$\alpha(\omega) = \frac{1}{3}\,\mathrm{Tr}\left[\overline{\alpha}(\omega)\right]. \quad (7)$$

It is well known that the simpler approach of taking the differences of eigenvalues between Kohn-Sham orbitals gives peaks at lower frequencies in disagreement with the experimental spectra [15]. On the other hand, TDDFT within the ALDA exchange-correlation functional typically produces the optical linear response of the molecular compound that is in good agreement with experimental results with accuracy below 0.2 eV.

3. Computational Detail

Hydrogen passivated silicon quantum dots (Si-QDs) with selected sizes up to 1.6 nm were constructed by repeating tetrahedral silicon geometry from its crystal geometrical structure (bulk structural properties) until the desired repetition was achieved. The prototype quantum dots are constructed in the order of quasi-spherical shape. Next, the quantum dots structures were passivated with hydrogen atoms on the surface. All the ground state relaxed structures were obtained after performing geometry optimization using the quasi-Newton method to get an ideal relaxation structure. The quasi-Newton method used is the Broyden-Fletcher-Goldfarb-Shanno (BFGS) method [16–19], all in Cartesian coordinates. This optimized structure is then used to calculate the electronic and optical properties, in particular the energy gap and absorption spectrum linear response. All the computational approaches were successfully done in real space and implemented using OCTOPUS [4]. The core electrons with strong coulombic effect were treated using the Troullier and Martins pseudo potentials [20] throughout this simulation. For the ground state calculation, the computational parameters used in our previous work were used exactly [5] to solve for the Kohn-Sham eigenvalues. Then the time-dependent calculations of the perturbed system were conducted. Subsequently, the time reversal symmetry propagator in the algorithms was used to approximate the evolution operator.

All linear response calculations were done using OCTOPUS [4] implementing the Perdew-Zunger [21] parameterization of the local density approximation (LDA) for the exchange-correlation potential. The wave functions representation in real space was mapped onto a uniform grid with a spacing of 0.175 Å and spheres of radius 4 Å around every atom. The system was perturbed by short electrical pulses $0.01\,\text{Å}^{-1}$. A time step of 0.0017 femtoseconds ensured the stability of the time propagation, and a total propagation time of 10 femtoseconds allowed a resolution of about 0.01 eV in the resulting energy spectrum with almost 6000 steps. The results obtained are summarized in Table 2 and also Figure 2 where the absorption spectrum was plotted for the whole perturbation.

4. Results and Discussion

4.1. Ground State Properties. At the beginning of this simulation, the accuracy of ground states calculation was examined by comparing the Kohn-Sham energy gaps obtained using different types of wave function representation and exchange-correlation function. This comparison acts as a benchmark for the simulation reliability of the selected parameter used. Table 1 shows the comparison of Kohn-Sham energy gaps (E_g, in eV) obtained from the ground state calculations of geometry optimized hydrogenated silicon quantum dots. Three different wave function representations were used to solve the Kohn-Sham equations, namely, the numerical atomic orbital (NAO), plane-waves (PWs), and real-space (RS) basis set. All the reported data were analyzed using the same computational approach (DFT) but in different wave function representation (PWs, NAO, and RS basis set) and exchange-correlation potential. Then, the approximated E_g values were checked. This calculation result using real-space method for the ground state eigenvalues is found to be in good agreement with others' theoretical report.

Before the absorption coefficient was calculated, attention was given first to the spatial distribution for the ground state of the HOMO and LUMO states. The results of the 3-dimensional spatial distribution for both states in different dot size are visualized in Figure 1. For larger sizes, it is noted

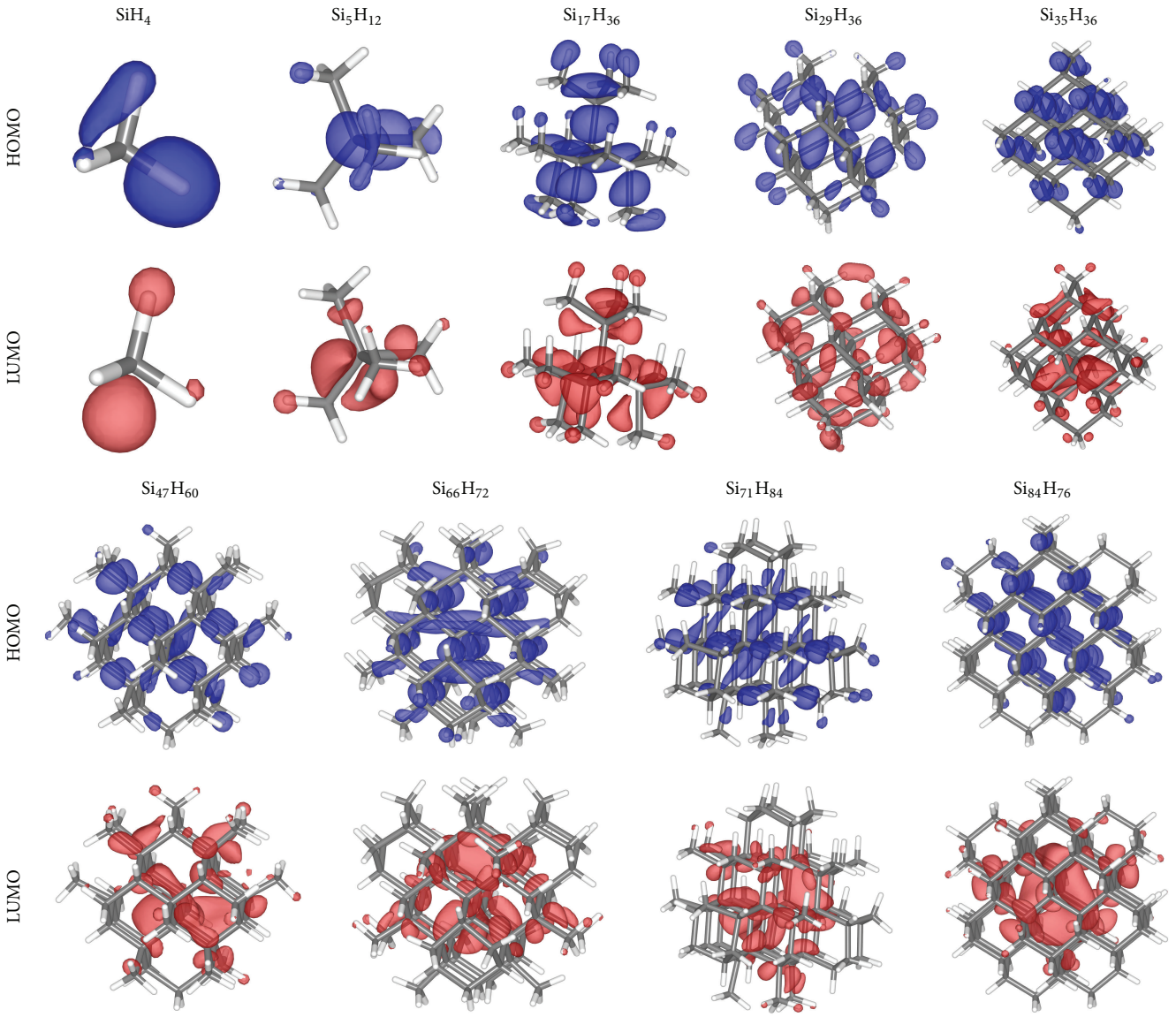

Figure 1: Spatial distribution of HOMO and LUMO plot.

Table 1: Comparison of ground state E_g (eV), calculated using different basis-set representation and exchange-correlation functional (∗ corresponding to $Si_{66}H_{64}$).

Quantum dots	NAO [5] (LDA) (without discontinuity correction)	PWs [6] (LDA)	PWs [7] (LDA)	RS [8] (B3LYP)	RS (LDA) (present study)
SiH_4	9.00	—	7.90	—	8.51
Si_5H_{12}	5.58	—	5.60	7.6	5.55
$Si_{17}H_{36}$	4.80	—	4.50	5.72	4.28
$Si_{29}H_{36}$	4.30	3.32	4.20	5.15	3.95
$Si_{35}H_{36}$	3.56	—	3.70	5.04	3.66
$Si_{47}H_{60}$	3.14	—	—	4.64	3.14
$Si_{66}H_{72}$	2.72	2.95*	2.8	—	2.73
$Si_{71}H_{84}$	2.70	—	—	4.20	3.0
$Si_{84}H_{76}$	2.51	—	2.5	—	2.54

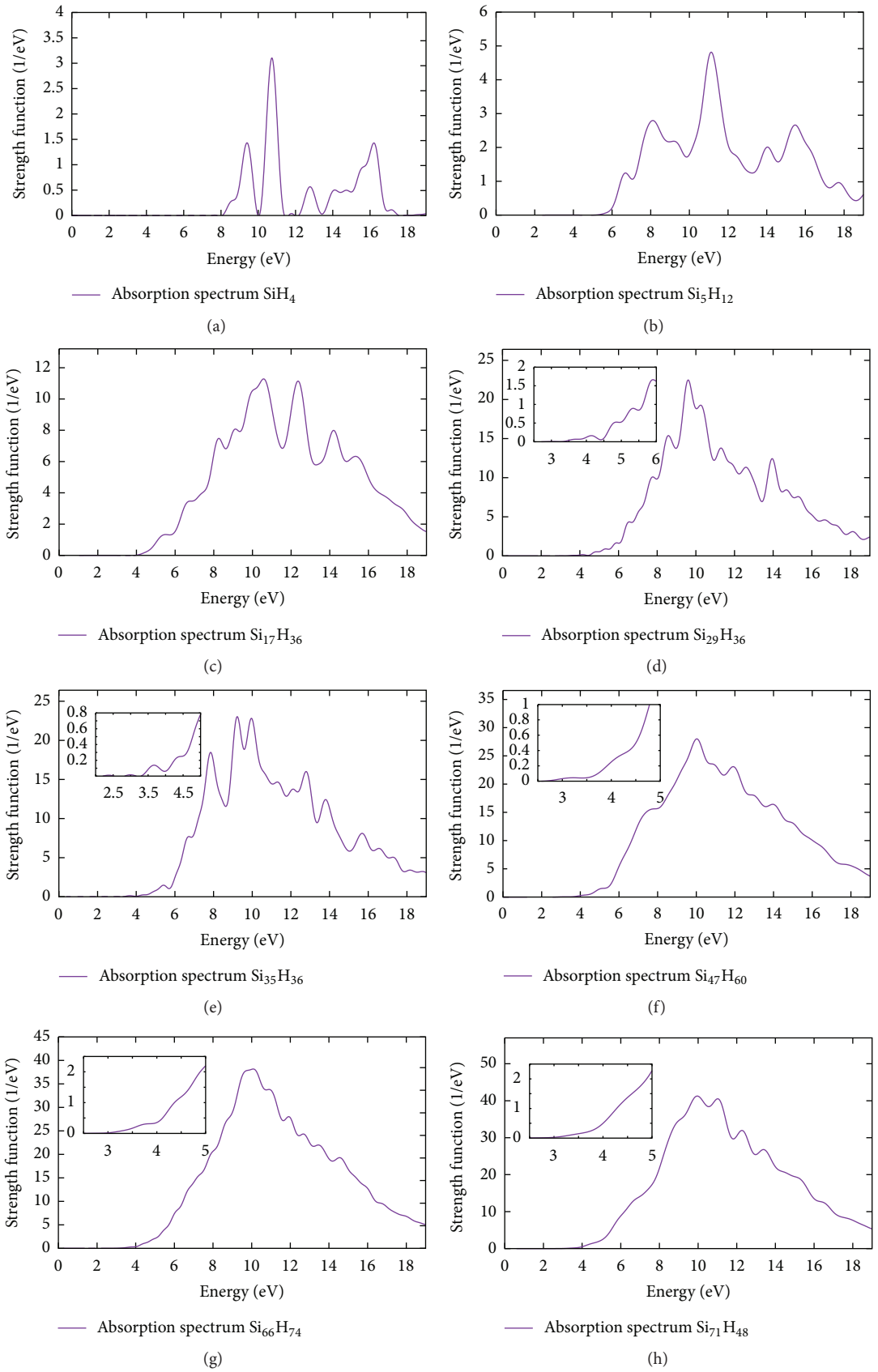

Figure 2: Continued.

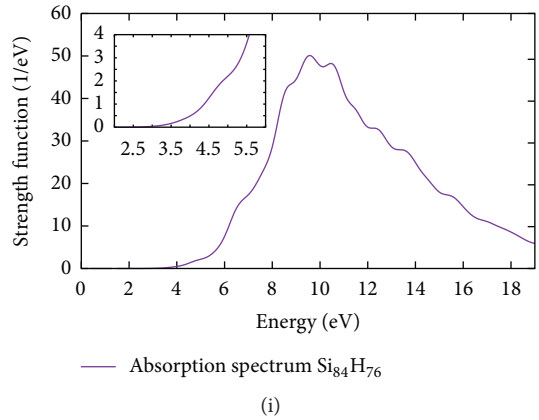

(i)

Figure 2: Optical absorption spectrum of hydrogenated silicon quantum dots.

Table 2: Comparison of results for optical properties [9–11].

Quantum dots		Optical properties		
Diameter (nm)	Empirical formula	Optical threshold (eV)	First noticeable peak (eV)	Second noticeable peak (eV)
—	SiH_4	8.1, 8.0 [9], 8.0 [11]	8.54, 8.7 [9], 8.2 [11]	9.45, 9.6 [9], 9.1 [11]
0.6	Si_5H_{12}	5.5, 5.7 [10], 5.6 [11]	6.7, 6.5 [10], 6.4 [11]	8.12
0.8	$Si_{17}H_{36}$	4.0	5.47	6.72
1.0	$Si_{29}H_{36}$	3.5	4.2	4.8
1.1	$Si_{35}H_{36}$	3.43	3.7	4.4
1.2	$Si_{47}H_{60}$	3.4	4.1	5.05
1.4	$Si_{66}H_{74}$	3.3	3.72	4.93
1.5	$Si_{71}H_{84}$	3.2	3.81	5.98
1.6	$Si_{87}H_{76}$	3.0	4.78	6.72

that the HOMO states are principally distributed along the direction of the bond axis and just a little on the surface states, whereas the LUMO states are located the other way around. It is also clearly seen that the surface distribution of the HOMO states contributes significantly to the value of the electronic property of energy gap. In contrast, the phenomena of phonon-assisted transition in bulk silicon make this element an ineffective purpose for optoelectronic devices. Their efficiency was reduced by phonon effect during electron transition in Brillouin zone. However, from spatial distribution of electron wave function shown in Figure 1, it was found that the probability of electron position in real space between HOMO and LUMO eigenstates was occupied in the same space. This will provide a direct transition of electron which can make silicon quantum dots a good candidate for future optoelectronic device.

Results in this study show that as the size increased, the nature of the localization of the HOMO and LUMO states differs from the smaller sizes and this obviously reflects the effect of the structural configuration on the electronic properties. It is clearly seen that hydrogen is bonded with silicon atoms even when its valance is one. This phenomenon can be elucidated from the electron spatial distribution isosurface of the HOMO and LUMO states for Si_5H_{12} (Figure 1). It can be seen clearly too that the HOMO exhibits a bonding character, where the electron cloud is predominantly located in the intermediate regions where the bonds are formed. On the other hand, the antibonding character of LUMO state is confirmed by the significant distribution of charge density at the vicinity of the atoms. For the largest quantum dot examined in this study, size around 1.6 nm diameter, the LUMO clearly shows its antibonding nature correspondingly. The HOMO displays a region of high density inside the QD as anticipated for 1s type (sphere) wave functions. It is inferred that, from the isosurface plots of HOMO and LUMO, the formation of the energy gap is originated from the localization of the electron cloud at the surface. The localization of both the HOMO and LUMO orbitals on hydrogen atoms illustrated that the gap is prominent and can be identified by hydrogen bonds, more clearly seen for smaller size quantum dots. In the nanostructures case, if a strong electronegativity difference is present between Si and the passivating atoms, the HOMO tends to concentrate (while preserving its delocalization) on the weakened surface Si–Si bonds. Hence, the surface states have different contribution for the HOMO and LUMO states. Also, the LUMO states indicate that the electrons are more localized near the hydrogen atoms. This situation is anticipated because there will be small charge transfer

from the silicon atoms to hydrogen. This may be attributed due to the slightly higher electronegativity of H atom as compared to Si atom. As a result, the H atom prefers to bond with the silicon atom which possesses a larger number of electrons. For silicon quantum dots, this can be at the cost of giving up the sp^3-hybridization. Therefore, the sp^3-character of diamond-like bulk materials may not be present in these small dots. As a matter of fact, the Pauling scale of electronegativity defined that silicon electronegativity is 1.9 while that of H is 2.2. If the bond considered is only between both elements (Si–H), then it can be considered as nonpolar, because the electronegativity difference between these two elements is 0.3. But, in this case of quantum dots study, the electron cloud from the core of the silicon atoms and the neighboring atom silicon-silicon charges contribute to increments of electronegativity differences which can be categorized as polar covalent bonding interaction. This is a clear explanation that the interaction between hydrogen and silicon leads not only to passivation of the dangling bonds, but also to alteration of the electronic properties of the silicon quantum dots.

4.2. Optical Properties. As the optical response of nanometer structures depends crucially on the particle size due to quantum effects, their optical properties can be tuned by changing their size, opening the road towards potential applications in optical nanodevices. Therefore it is important to have a reliable scheme to address the calculation of response functions. In the case of nonlinear phenomena, the present exchange-correlation functional might not be highly accurate, but they nevertheless yield relevant information about the systems. Again, all of the results reported have been obtained using the OCTOPUS code based on real-space method of wave function representation.

In order to interpret the absorption spectrum of various sized silicon quantum dots, let us take the absorption edge as the energy threshold, opening gap of absorption spectra. It is well known that the optical gap is different from the energy gap calculated from differences energy level of HOMO and LUMO, where $E_{\text{gap}} = E_{\text{HOMO}} - E_{\text{LUMO}}$, because the first allowed excitation is often too weak to be detected. For a meaningful comparison with experiment, the same empirical criterion employed in interpreting experimental data which is related to the detection of the absorption threshold was used and the first two absorption peaks were detected [9, 10]. The conformity of these time-dependent calculations was checked by comparing these results with the experimental results for SiH_4 (silane) and Si_5H_{12}. It is observed that the first peak of silane optical threshold resulting in this simulation is 8.10 eV, and the first peak is 8.54 eV. Meanwhile, for Si_5H_{12} the optical threshold is 5.45 eV; the first allowed transition peak was observed at 6.7 eV as shown in Figures 2(a) and 2(b). On the other hand, the experimental value reported that the onset of absorption spectrum for silane was 8 eV, and the first peak observed was around 8.7 eV [9]. Experimental optical threshold and the first peak observed for Si_5H_{12} were 5.7 eV and 6.53 eV, respectively [10]. These experimental results are in good agreement with our calculated results, with small errors between 0.1 and 0.2 eV. This benchmark indicates that this conducted study is in a right way, as its results are close to the reported experimental values. Subsequently this simulation is extended to study the absorption spectra of larger quasi-spherical silicon quantum dots with diameter up to 1.6 nm.

For the structure with the largest diameter ($Si_{87}H_{76}$), the first noticeable transition peak was detected close to 5.0 eV (see Figure 2(i)). The presence of a very small numerical noise was also noticed on the left side of the optical threshold observed for $Si_{35}H_{36}$ structure. Those noise peaks occupy very small oscillator strength which can be neglected from the characteristic of prominent optical absorption. A distribution of an absorption peak in the optical absorption versus photon energy curve denotes that increments of photon absorption begin from 4 to 11 eV with noticeable peaks which infers that there is an important absorption of photons at this region for Si nanostructures which is different from bulk Si. Other intriguing characteristics that also can be noticed are that the highest absorption peak of nanosized structure was shifted towards higher energy level, where the highest absorption peak for silicon quantum dots was located around 11 eV. This differs from the experimental determinations of bulk silicon optical properties where the main peak (highest peak) occurrence of the photon absorption is at energy around 4.3 eV [22] that indicates the electron confinement phenomena much higher in nanosized structure. The calculated optical gaps as identified from these absorption spectra are shown in Table 2 and compared with experimental and previously reported values.

The obtained calculation results infer that the surface effects caused by the single bonded passivators participate in the optical transitions. It is obvious to understand that with the increment of dot size both the energy gap and optical gap are reduced because of deconfinement effect. According to the exciton de Broglie wavelength for silicon, the effective diameter of silicon quantum dots where the confinement effect will affect its electronic properties should be below 5 nm [23]. This specific tendency of tuneable sizes that produce the variation of energy gap makes the silicon a new candidate for optoelectronic devices. Despite its excellent character of tuneable wavelengths from ultraviolet to infrared, silicon quantum dots were biofriendly element and nontoxic element to use in biological living.

It is noticed that, for all the silicon quantum dots considered, their optical gap is higher than the correspondingly ground state Kohn-Sham energy gap. It is inferred that this occurrence was caused by the allowed excitation transition state of electron from HOMO to LUMO state with reasonable oscillator strength. The absorption spectra for smaller dots illustrate a combination of many peaks and resemble isolated atoms. While on a larger Si-QD, the overlap between the electronic wave functions removes the nondegeneracy of the energetic states that arises in the grouping of energy states in a narrow energy section. This induces broadening of width and increment of the absorption oscillator strength for larger nanostructures. A red shift of the optical absorption spectrum is found to appear with the increment in the dot diameter of silicon quantum dots. In larger dots (1.6 nm), the major feature (maximum peak) of the absorption spectra is

located around 9.8 eV and the declination feature begins to appear after 11 eV.

5. Conclusion

The electronic structure and absorption coefficients of hydrogenated silicon quantum dots have been calculated using time-dependent density functional theory. Calculations in this study showed a very good and significant agreement for the benchmark small silicon quantum dots of SiH_4 and Si_5H_{12} with earlier theoretical calculations and experimental results. It is found that the changes in the photoabsorption spectra correlate well with the changes in the size of the quantum dots. For relatively large hydrogenated silicon quantum dots (1.6 nm), it shows bulk-like behavior with smooth noticeable peak, while for the small structure the absorption spectra are composed of numerous peaks as in isolated atoms. It is found that the optical gap for the large structure, with diameter around 1–1.6 nm, is suitable for optoelectronic application, where its first peak of absorption is observed around 3.7 to 5 eV which lies under ultraviolet region. The optical gap decreases gradually with the increase in number of silicon atoms in the quantum dots. The absorption spectra display significant red shifts with respect to the increment size of dot. This phenomenon is due to deconfinement effect of electrons trapped in quantum dots. The calculated spectra present varieties of features that could be used for structure identification. It is noticed that the TDDFT computed optical threshold differs significantly from energy gap simply computed from difference of ground state energy level of HOMO-LUMO which can provide much better approximation of energy gap using TDDFT calculation. The significant absorption threshold obtained can be used to classify the character and structure, precisely up to 0.1 nm in difference. It is also confirmed that LDA functional in TDDFT calculation method predicts good approximation for the optical gap of low-dimensional structures, where the obtained results are very consistent with the absorption spectrum reported by the experiment.

Conflict of Interests

The authors declared that there is no conflict of interests regarding the publication of this paper.

Acknowledgments

The authors would like to thank the Malaysian Ministry of Science, Technology and Innovation (MOSTI) for Science Fund Funding 06-01-02-SF0988 and Malaysian Ministry of Education Scholarship (MyBrain15) to Muhammad Mus-'ab Anas.

References

[1] J. Zeng and H. Yu, "A first-principle study of B- and P-doped silicon quantum dots," *Journal of Nanomaterials*, vol. 2012, Article ID 147169, 7 pages, 2012.

[2] E. Runge and E. K. U. Gross, "Density-functional theory for time-dependent systems," *Physical Review Letters*, vol. 52, no. 12, pp. 997–1000, 1984.

[3] E. K. U. Gross and W. Kohn, "Local density-functional theory of frequency-dependent linear response," *Physical Review Letters*, vol. 55, no. 26, pp. 2850–2852, 1985.

[4] M. A. L. Marques, A. Castro, G. F. Bertsch, and A. Rubio, "Octopus: a first-principles tool for excited electron–ion dynamics," *Computer Physics Communications*, vol. 151, no. 1, pp. 60–78, 2003.

[5] M. M. Anas, A. P. Othman, and G. Gopir, "First-principle study of quantum confinement effect on small sized silicon quantum dots using density-functional theory," *AIP Conference Proceedings*, vol. 1614, pp. 104–109, 2014.

[6] M. Hirao and T. Uda, "Electronic structure and optical properties of hydrogenated silicon clusters," *Surface Science*, vol. 306, no. 1-2, pp. 87–92, 1994.

[7] A. J. Williamson, J. C. Grossman, R. Q. Hood, A. Puzder, and G. Galli, "Quantum Monte Carlo calculations of nanostructure optical gaps: application to silicon quantum dots," *Physical Review Letters*, vol. 89, no. 19, Article ID 196803, 4 pages, 2002.

[8] A. D. Zdetsis, C. S. Garoufalis, and S. Grimme, "Real space *Ab initio* calculations of excitation energies in small silicon quantum dots," in *Quantum Dots: Fundamentals, Applications, and Frontiers*, vol. 190 of *NATO Science Series*, pp. 317–332, Springer, Dordrecht, The Netherlands, 2005.

[9] U. Itoh, Y. Yasutake, H. Onuki, N. Washida, and T. Ibuki, "Vacuum ultraviolet absorption cross sections of SiH_4, GeH_4, Si_2H_6, and Si_3H_8," *The Journal of Chemical Physics*, vol. 85, no. 9, pp. 4867–4872, 1986.

[10] F. Fehér, *Molekülspektroskopische Untersuchungen auf dem Gebiet der Silane und der Heterocyclischen Sulfane*, Forschungsberichtdes Landes Nordrhein-Westfalen, Westdeutscher, Cologne, German, 1977.

[11] J. Thingna, R. Prasad, and S. Auluck, "Photo-absorption spectra of small hydrogenated silicon clusters using the time-dependent density functional theory," *Journal of Physics & Chemistry of Solids*, vol. 72, no. 9, pp. 1096–1100, 2011.

[12] G. Onida and W. Andreoni, "Effect of size and geometry on the electronic properties of small hydrogenated silicon clusters," *Chemical Physics Letters*, vol. 243, no. 1-2, pp. 183–189, 1995.

[13] X. Xue Jiang, J. Zhao, and X. Jiang, "Tuning the electronic and optical properties of hydrogen-terminated Si nanocluster by uniaxial compression," *Journal of Nanoparticle Research*, vol. 14, article 818, 10 pages, 2012.

[14] I. Vasiliev, "Optical excitations in small hydrogenated silicon clusters: comparison of theory and experiment," *Physica Status Solidi*, vol. 239, no. 1, pp. 19–25, 2003.

[15] A. Castro, M. A. L. Marques, J. A. Alonso, G. F. Bertsch, K. Yabana, and A. Rubio, "Can optical spectroscopy directly elucidate the ground state of C20?" *Journal of Chemical Physics*, vol. 116, no. 5, pp. 1930–1933, 2002.

[16] C. G. Broyden, "The convergence of a class of double-rank minimization algorithms 1. General considerations," *Journal of the Institute of Mathematics and Its Applications*, vol. 6, no. 1, pp. 76–90, 1970.

[17] R. Fletcher, "New approach to variable metric algorithms," *Computer Journal*, vol. 13, no. 3, pp. 317–322, 1970.

[18] D. Goldfarb, "A family of variable-metric methods derived by variational means," *Mathematics of Computation*, vol. 24, pp. 23–26, 1970.

[19] D. F. Shanno, "Conditioning of quasi-Newton methods for function minimization," *Mathematics of Computation*, vol. 24, no. 111, pp. 647–656, 1970.

[20] N. Troullier and J. L. Martins, "Efficient pseudopotentials for plane-wave calculations," *Physical Review B*, vol. 43, no. 3, pp. 1993–2006, 1991.

[21] J. P. Perdew and A. Zunger, "Self-interaction correction to density-functional approximations for many-electron systems," *Physical Review B*, vol. 23, no. 10, pp. 5048–5079, 1981.

[22] H. R. Philipp and E. A. Taft, "Optical constants of silicon in the region 1 to 10 ev," *Physical Review*, vol. 120, no. 1, pp. 37–38, 1960.

[23] C. S. Solanki, *Solar Photovoltaics: Fundamentals Technologies and Applications*, Prentice-Hall of India, New Delhi, India, 2009.